

# First Evidence of Light-induced Spin Transition in Molybdenum(IV)

*Nathalie Bridonneau, Jérôme Long, Jean-Louis Cantin, Jurgen von Bardeleben Sébastien Pillet, El-Eulmi Bendeif, Daniel Aravena, Elizeo Ruiz, and Valérie Marvaud\**

## Supplementary Information

<b>1- Experimental Section</b>	<b>p 2</b>
<b>2- EPR measurements</b>	<b>p 2</b>
<b>3- X-ray analyses under irradiation</b>	<b>p 3-5 Figures S1, Table S1-S2</b>
<b>4- Photomagnetic measurements</b>	<b>p 6 Figures S2-S3</b>
<b>5- Calculations</b>	<b>p 7</b>
<b>6- IR studies</b>	<b>p 7-8 Figures S4-S5</b>
<b>7- XMCD measurements</b>	<b>p 9</b>
<b>References</b>	<b>p 9</b>

## 1- Experimental Section

**Synthesis of MoZn<sub>2</sub>-tren (1)** [Mo(CN)<sub>6</sub> {(μ-CN)ZnC<sub>6</sub>H<sub>18</sub>N<sub>4</sub>}<sub>2</sub>]. (H<sub>2</sub>O)<sub>10</sub>

Caution! Cyanides are very toxic and must be handled with care.

83 mg of tren ligand (Tris(2-aminoethylamine, 0.56 mmol, 4 eq.) dissolved in water/acetonitrile (1:1, 10 mL) were added to a solution of [Zn(OAc)<sub>2</sub>]•2H<sub>2</sub>O (purity 99.999 %, 124 mg, 0.56 mmol, 4 eq.) in the same solvent mixture. The solution was stirred for a few minutes before adding carefully (dropwise) a solution of K<sub>4</sub>[Mo<sup>IV</sup>(CN)<sub>8</sub>]•2H<sub>2</sub>O (70 mg, 0.14 mmol, 1 eq.) without agitation. The solution is filtrated then left for slow evaporation in the dark. Yellow crystals were obtained within a week.

Yield: 80 %. IR (KBr, cm<sup>-1</sup>): 3200, 2950, 2147, 2121, 2107, 2098, 1602, 1456.

Anal Calc for MoZn<sub>2</sub>C<sub>20</sub>H<sub>56</sub>N<sub>16</sub>O<sub>20</sub>: Mo 12.14, Zn 16.55, C 30.39, H 28.35, N 5.48, Found: Mo 12.15, Zn 16.94, C 30.49, H 28.09, N 5.28.

## 2- EPR measurements

**EPR measurements** were performed on a single crystal with a standard X-band spectrometer and a 4–300 K variable temperature cryostat under irradiation. EPR measurements were performed with a Bruker ESP 300 spectrometer, at X Band frequency (9.5GHz). The magnetic field modulation frequency was set at 100 kHz and the modulation amplitude and the microwave power were both adjusted to avoid saturation. The spectra were measured at temperatures between 4 K and 300 K. The excitation of the samples at low temperature was performed with laser sources at 405 and 488 nm.

EPR measurements were done on single crystals of **1** prepared with and without *purissime* Zinc acetate (99.99 and 99.999%) but we observed in all cases contamination by copper species. Before irradiation, no relevant signal was detected, as expected for diamagnetic species (except a tiny amount of Cu(II)). Upon light irradiation at 4 K (using 405 or 488 nm laser beams) large signals appeared, including in the half field range (1000 – 2200 Oe).<sup>S1</sup> Unfortunately, despite all our efforts, no signal can be formally attributed to forbidden transition ( $\Delta M_s = \pm 2$ ) that we might expect for a triplet species generated by the photo-induced spin transition in the molybdenum center: Mo<sup>IV</sup><sub>LS</sub> (S = 0) → Mo<sup>IV</sup><sub>HS</sub> (S = 1).<sup>S2</sup> Simulation is not trivial for half-field transition as confirmed by reference S2. It is not as simple as describing the triplet species on Mo and hyperfine splitting. Analysis of data at two microwave frequencies may be required to obtain definitive results. Experiments are in progress.

Heating the compound gradually produced the disappearance of the photo-induced signals, clearly indicating the reversibility of the process.

### **3- X-ray crystal structure analyses**

**X-ray crystal structure analyses** were conducted on crystals directly obtained from the reaction medium. Data were collected on a Microfocus Supernova diffractometer equipped with a two dimensional ATLAS detector, using Mo K $\alpha$  radiation ( $\lambda = 0.71073 \text{ \AA}$ ), and a Helijet He open flow cryosystem. The temperature was fixed at 10 K. Diffraction data were first collected at 10 K in the ground state (GS) using  $\omega$ -scans. The unit cell determination and data reduction were performed using the *CrysAlis* program suite (Oxford Diffraction, 2011) on the full data set. 86033 reflections were measured up to a maximum resolution of  $\theta_{\text{max}} = 31.51^\circ$ , and merged to 21669 unique reflections ( $R_{\text{int}} = 0.0453$ ). Numerical absorption correction was performed. The corresponding structure was solved in the *Pca2<sub>1</sub>* space group by direct methods with the SHELXS97 program (Sheldrick, 2008) and refined on  $F^2$  by weighted full matrix least-squares methods using the SHELXL97 program (Sheldrick, 2008). All non-hydrogen atoms were refined anisotropically, hydrogen atoms were generated at their ideal position and treated using a riding model, constraining the isotropic displacement parameters to 1.2 times those of the attached C atom. Hydrogen atoms of water molecules were not located in difference Fourier maps.

#### ***XRD under irradiation***

A fresh second sample was selected, and irradiated at 10 K with a diode laser at 405 nm ( $P = 70 \text{ mW}$ ) during 30 min, before observing a severe amorphisation of the sample. This laser exposure time is a compromise between photo-conversion efficiency and amorphisation. Photo-difference maps have been calculated for visualisation of the light-induced changes in electron density, and identification of the related structural changes from the GS to the excited state (Figure S1). Common independent reflections between the GS and photo-irradiated state have been used to compute the experimental X-ray photo-difference map by Fourier transform of the difference ( $F_{\text{photo-irradiated}}^{\text{obs}}(hkl) - F_{\text{GS}}^{\text{obs}}(hkl)$ ), using the structure factor phases from the GS structural refinement. The calculated photo-difference map reveals some structural reorganisation. For the Mo1 molecule, this map displays electron deficient regions (red coloured) centred on the position of the heaviest atoms in the ground state (Mo1, Zn2, Zn1), and an electron density accumulations (blue coloured) around Mo1. This corresponds mainly to an increase of atomic displacement parameters (atomic disorder) in the photo-irradiated state. On the contrary, for the second molecule, the map highlights a slight displacement of the Mo2 and Zn4 atoms in the photo-irradiated state, as evidenced by electron deficient regions (red coloured) centred on the position of the atoms together with adjacent electron density accumulations (blue coloured) not centred on the atomic position. We can conclude that in the photo-irradiated state, only the atoms Mo2 and Zn4 undergo a significant displacement. This displacement occurs in the opposite direction, corresponding to an increase of the Mo2...Zn4 distance.

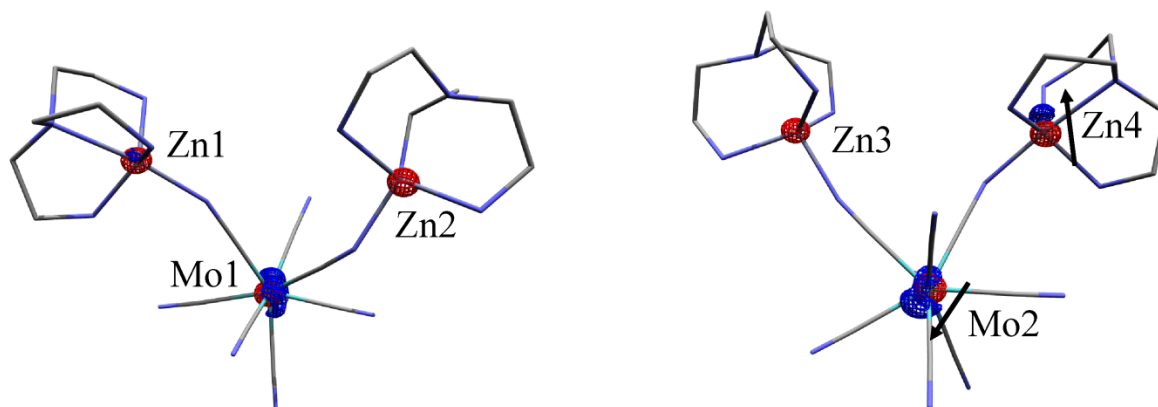


**Figure S1.** 3D photo-difference map with isosurface of  $\pm 8.0 \text{ e}\text{\AA}^{-3}$  (red, negative; blue, positive) at 10 K after irradiation with 405 nm. Arrows indicate the putative atomic displacement in the photo-irradiated state.

Interatomic distances ( $\text{\AA}$ )		Angles ( $^\circ$ )	
Mo1-C	2.135(3)-2.165(4)	Mo1-C-N(cyano)	175.6(3)-178.5(3)
Mo2-C	2.152(3)-2.182(4)	Mo1-C-N(free)	175.1(3)-178.7(3)
free C-N	1.147(4)-1.165(4)	Mo2-C-N(cyano)	176.8(3)-177.5(3)
Zn-N(tren)	2.035(3)-2.285(3)	Mo2-C-N(free)	176.8(3)-178.0(3)
Zn-N(cyano)	2.050(3)-2.105(3)	C-N-Zn1	157.1(3)
Mo1...Mo2	10.0981(4)	C-N-Zn2	145.3(3)
Zn1...Zn2	6.4885(6)	C-N-Zn3	165.0(3)
Zn3...Zn4	6.4469(6)	C-N-Zn4	137.1(3)
Mo1...(Zn1,Zn2)	5.2431(4)-5.0692(5)	C1-Mo1-C2	77.90(14)
Mo2...(Zn3,Zn4)	5.3246(4)-5.0383(5)	C9-Mo2-C10	75.12(12)

**Table S1:** Table of main distances and angles of **1**

The photo-irradiated state crystal structure corresponds to an average structure with a mixture of ground state and photo-irradiated state molecular species. Attempts to deconvolute the two configurations were unsuccessful.

	Ground state	Photo-irradiated state (30 min)
<i>T</i> /K	10	10
Crystal System	orthorhombic	orthorhombic
Space group	Pca21	Pca21
<i>a</i> / Å	14.7778(3)	14.8514(3)
<i>b</i> / Å	14.8566(3)	14.9939(3)
<i>c</i> / Å	31.0576(7)	31.0699(7)
<i>V</i> / Å <sup>3</sup>	6818.6(2)	6918.6(3)
<i>Z</i>	4	4
Measured data	86033	76836
$\Theta_{max}$	31,51	31,51
<i>R</i> <sub>int</sub>	0.0453	0.0759
$\mu$ / mm <sup>-1</sup>	1,814	1,814
<i>T</i> <sub>min</sub> / <i>T</i> <sub>max</sub>	0,606 / 0,724	0,541 / 0,661
Independent data	21669	21900
<i>R</i> 1 [ <i>F</i> <sup>2</sup> > 2 <i>s</i> ( <i>F</i> <sup>2</sup> )]	0.0415 [0.0381]	0.1167 [0.0911]
<i>wR</i> 2 [ <i>F</i> <sup>2</sup> > 2 <i>s</i> ( <i>F</i> <sup>2</sup> )]	0.0947 [0.0917]	0.2468 [0.2221]

**Table S2:** Evolution of the crystallographic and refinement details of **1** after irradiation

#### 4- Photomagnetic measurements

**Photomagnetic measurements.** DC magnetic susceptibility measurements were carried out on a Quantum Design MPMS SQUID susceptometer equipped with a 7 T magnet and operating in the 1.8 K – 400 K range. The SQUID is equipped with a fiber connected to a 405 nm laser. For the photomagnetic experiments samples are deposited as crystals or grounded powder on a film located at approximately 2 cm from the fiber. Samples were typically irradiated at 10 K under a 1kOe field for a few hours (approx. 3h30) until saturation of the signal was observed. The temperature was then decreased to 2 K and magnetic data recorded on the heating mode (under a 500 Oe or 1000 Oe field). To check the reversibility of the process, the same workup was applied, then the compound was kept a few hours at room temperature (typically 3 h) and the magnetic data were recorded again in the 300 K – 2 K range.

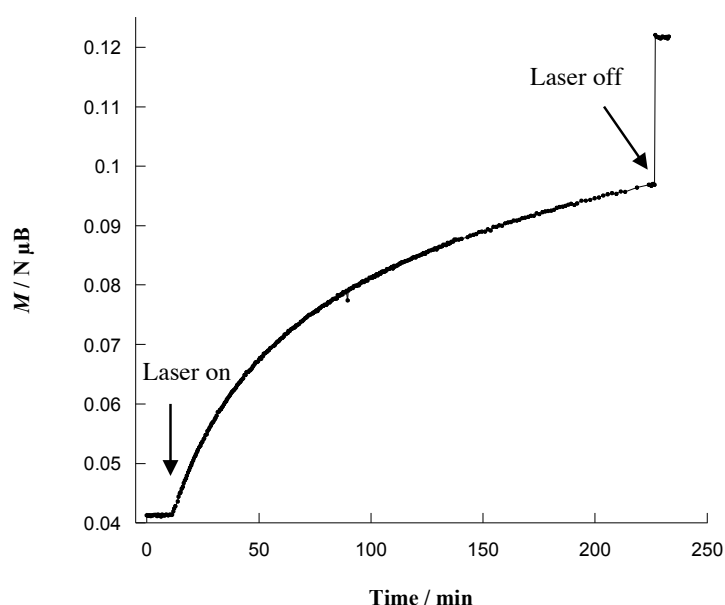


**Figure S2:** Evolution of the magnetization of **1** upon light irradiation at 18 K ( $H = 1\text{T}$ ).

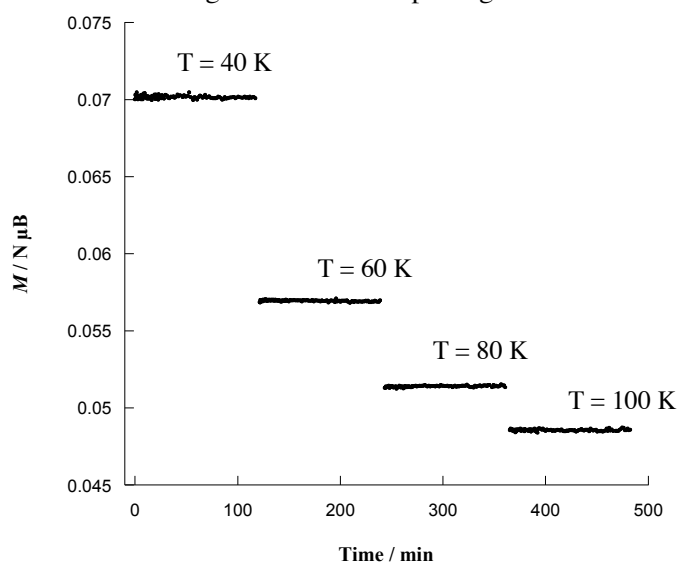


**Figure S3:** Stability of the photoinduced state of **1**,  $H = 5\text{T}$

## **5- Calculations**

**Electronic Structure Calculations.** CASSCF(2,5) calculations were performed with the Molcas 7.8 code<sup>S3</sup>; dynamic correlation effects were perturbatively added with the CASPT2 method (basis sets: Mo.ANO-RCC-7s6p4d2f1g, N.ANO-RCC-4s3p2d1f, C.ANO-RCC-4s3p2d1f and H.ANO-RCC-2s) all the 10 triplets and 15 singlets were included. DFT calculations were carried out using the Gaussian09 D.1 code<sup>S4</sup> using the hybrid B3LYP functional<sup>S5</sup> and the Def2TZVP basis set.<sup>S6</sup>

## **6- Infra-Red Studies** at low temperature (10K), under irradiation (488 nm):

Cyanide compounds have some advantages as an infrared ligand probe. Owing to the variation of electrons to the (anti)bonding orbitals, it can be ascertained that  $\nu(\text{CN})$  values gives information on the metal oxidation state and coordination number. Infrared spectra have been recorded at low temperature (10 K), under irradiation (488 nm) and the spectra indicate a decrease of intensity of the base bands at 2155, 2127, 2112, 2099  $\text{cm}^{-1}$  as well as the apparition of a new band at 2178  $\text{cm}^{-1}$  as depicted in Figure 5 (see details in SI and figure S4), in good agreement with the evolution of the oxidation state of the molybdenum. After thermal relaxation of the compound, the initial spectrum is fully recovered.

IR spectra were recorded as KBr pellets on a Bio-Rad Win-IR FTS 165 spectrometer (250 – 4000  $\text{cm}^{-1}$ , 4  $\text{cm}^{-1}$  resolution). Infra-Red Studies at low temperature (10 K), under irradiation (488 nm) were collected using a Nicolet 5700 FTIR spectrometer with a resolution of 2  $\text{cm}^{-1}$ . The samples were finely ground, mixed with KBr, and pressed to pellets. To ensure good thermal contact for the low-temperature measurements, the pellets were contacted with silver paste on the cold finger of a home-built cryostat. The samples were cooled to liquid helium temperature (10 K) in the evacuated sample chamber (106 mbar). The cryostat is equipped with CsI windows allowing for collection of spectra in the range 8000–260  $\text{cm}^{-1}$  and for in situ illumination with lasers. The excitation of the samples at low temperature was performed with different laser sources with wavelengths ranging from 325 nm up to 1064 nm. In the present studies the experiments have been performed with 405 and 488 nm.

The compound  $\text{MoZn}_2$  (**1**) has been characterized by Infra-Red spectroscopy. Before irradiation, at room temperature, in the frequency range of 2000–2200  $\text{cm}^{-1}$ , the large asymmetric stretching bands of cyanide  $\text{CN}^-$  are observed at 2098, 2107, 2121 and 2147  $\text{cm}^{-1}$  attributed to terminal and bridging cyanide ligands of Mo(IV-LS). As the temperature decreases, from 300K to 10K, the CN stretching band shifts to higher frequencies (2099, 2112, 2127 and 2155  $\text{cm}^{-1}$ ). The intensities of all these peaks decreased after partial irradiation of the sample, but a new peak appears at 2178  $\text{cm}^{-1}$  attributed to bridging cyanide ligand between Mo(IV-HS) and Zn(II) (figure S5).

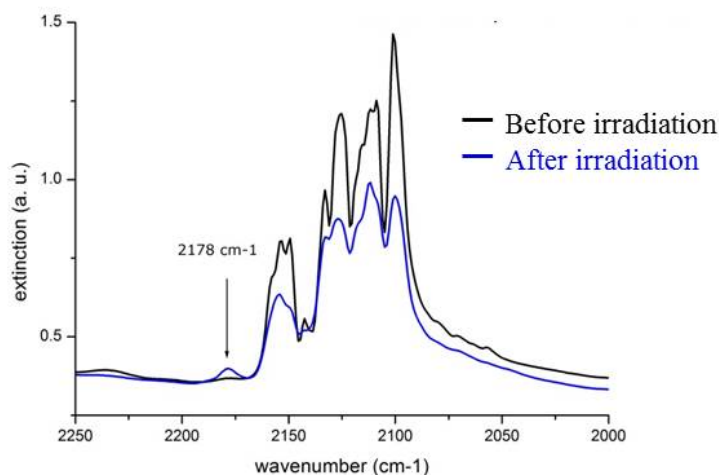


**Figure S4.** Evolution of the spectrum of **1** upon irradiation: black (before irradiation), blue (after irradiation, 488nm, 10 mn, 10 K). Zoom over the cyanide range (2000-2500  $\text{cm}^{-1}$ ).

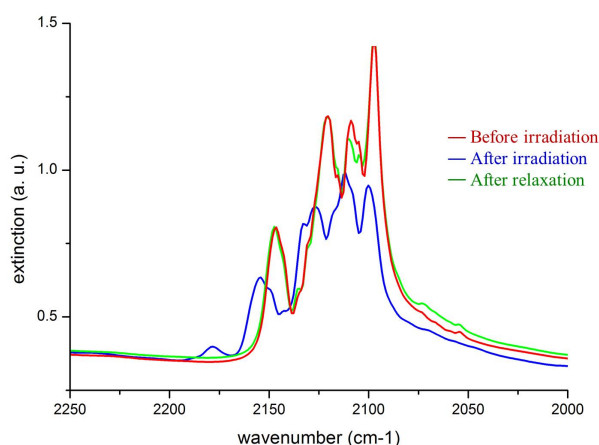


**Figure S5.** Test of reversibility: red (before irradiation, r. t.), blue (after irradiation, 488nm, 10 mn, 10K), green (after irradiation, r. t.). Zoom over the cyanide range (2000-2500  $\text{cm}^{-1}$ )

There is no reference spectra in the literature for high spin Mo(IV) or Mo(V)Zn(II) compounds, but Mo(V)Cu(II) species exist and exhibit cyanide stretching band at about  $2183 \text{ cm}^{-1}$  at room temperature. It is well known that the spectra of the octacyanomolydate with divalent metals show significant shift to higher frequencies relative to the principal band of  $[\text{Mo}(\text{CN})_8]^{4-}$ .<sup>S7</sup> The greatest shift is found for the  $\text{Zn}^{2+}$  compounds and the shift appears to decrease continuously across the transition series from  $\text{Zn}^{2+}$  to  $\text{Mn}^{2+}$ . Taking into consideration such argument and the shift due to the temperature, we may suggest that the peak observed at  $2179 \text{ cm}^{-1}$  is ascribed to a bridging cyanide ligand between Mo(IV-HS) and Zn(II). After thermal relaxation, the initial spectrum has been recovered indicating the reversibility of the process (Figure 6, green curve). This confirms that there is no release of the cyanide ligand.

## 7- XMCD measurements

The molecule has been investigated by X-ray magnetic circular dichroism (XMCD) measurements at the Molybdenum L<sub>2,3</sub> edges and the results are very similar to the one already obtained in previous work concerning MoCu species<sup>6</sup> and will be fully published elsewhere. Before irradiation, no XMCD signal was observed as expected for diamagnetic species. After 3h of irradiation of the compound ( $\lambda = 405$  nm), we noticed the appearance of a new band situated at 2521.1 eV corresponding to a 2p  $\rightarrow$  4s transition, correlated to a XMCD signal indicating presence of spin density on the molybdenum. Reversibility of the process was attested by the almost complete recovery of the initial signal as the compound was brought back to room temperature, in association with the disappearance of the XMCD signal.

These experiments confirm that the oxidation state of the compound is unchanged after irradiation, and are in agreement with the formation of a S = 1 compound, giving an additional argument to the formation of Mo<sup>IV</sup><sub>HS</sub> (S = 1) species.<sup>S8</sup>

## References

- <sup>S1</sup> N. Bridonneau, *PhD thesis UPMC*, Paris 6, France, 2013.
- <sup>S2</sup> P. Bertrand, *La Spectroscopie de Résonance Paramagnétique Electronique*, EDP Science, 2010, **ISBN-10: 2759805549**.
- <sup>S3</sup> F. Aquilante, L. De Vico, N. Ferre, G. Ghigo, P. A. Malmqvist, P. Neogady, T. B. Pedersen, M. Pitonak, M. Reiher, B. O. Roos, L. Serrano-Andres, M. Urban, V. Veryazov, R. Lindh, *J. Comput. Chem.* 2010, **31**, 224.
- <sup>S4</sup> M. J. Frisch, G. W. Trucks, H. B. Schlegel, G. E. Scuseria, M. A. Robb, J. R. Cheeseman, G. Scalmani, V. Barone, B. Mennucci, G. A. Petersson, H. Nakatsuji, M. Caricato, X. Li, H. P. Hratchian, A. F. Izmaylov, J. Bloino, G. Zheng, J. L. Sonnenberg, M. Hada, M. Ehara, K. Toyota, R. Fukuda, J. Hasegawa, M. Ishida, T. Nakajima, Y. Honda, O. Kitao, H. Nakai, T. Vreven, J. Montgomery, J. A., J. E. Peralta, F. Ogliaro, M. Bearpark, J. J. Heyd, E. Brothers, K. N. Kudin, V. N. Staroverov, R. Kobayashi, J. Normand, K. Raghavachari, A. Rendell, J. C. Burant, S. S. Iyengar, J. Tomasi, M. Cossi, N. Rega, N. J. Millam, M. Klene, J. E. Knox, J. B. Cross, V. Bakken, C. Adamo, J. Jaramillo, R. Gomperts, R. E. Stratmann, O. Yazyev, A. J. Austin, R. Cammi, C. Pomelli, J. W. Ochterski, R. L. Martin, K. Morokuma, V. G. Zakrzewski, G. A. Voth, P. Salvador, J. J. Dannenberg, S. Dapprich, A. D. Daniels, Ö. Farkas, J. B. Foresman, J. V. Ortiz, J. Cioslowski, D. J. Fox, Wallingford, CT, **2009**.
- <sup>S5</sup> A. D. Becke, *J. Chem. Phys.* 1993, **98**, 5648.
- <sup>S6</sup> F. Weigend, R. Ahlrichs, *Phys. Chem. Chem. Phys.* 2005, **7**, 3297; F. Weigend, *Phys. Chem. Chem. Phys.*, 2006, **8**, 1057.
- <sup>S7</sup> G. F. McKnight, G.P.Haight, *Inorg. Chem.*, 1973, **12**, 3007.
- <sup>S8</sup> a) M.-A. Arrio, J. Long, C. Cartier dit Moulin, A. Bachschmidt, V. Marvaud, A. Rogalev, C. Mathoniere, F. Wilhelm, P. Saintavit, *Jour. of Phys. Chem. C*, 2010, **114**, 593; b) S. Brossard, F. Volatron, L. Lisnard, M.-A. Arrio, L. Catala, C. Mathoniere, T. Mallah, C. Cartier dit Moulin, A. Rogalev, A. Smekhova, P. Saintavit, *J. Am. Chem. Soc.*, 2012, **134**, 222.